



The mitochondrial protease ClpP is a druggable target that controls VSMC phenotype by a SIRT1-dependent mechanism

Felipe Paredes^a, Holly C. Williams^a, Xuesong Liu^{a,b}, Claire Holden^a, Bethany Bogan^a, Yu Wang^a, Kathryn M. Crotty^{c,d}, Samantha M. Yeligar^{c,d}, Alvaro A. Elorza^e, Zhiyong Lin^a, Amir Rezvan^a, Alejandra San Martin^{a,e,*}

^a Department of Medicine, Division of Cardiology, Emory University, Atlanta, GA, United States

^b Department of Cardiology, The First Affiliated Hospital of Kunming Medical University, Kunming, China

^c Department of Medicine, Division of Pulmonary, Allergy, Critical Care and Sleep Medicine, Emory University, Atlanta, GA, United States

^d Atlanta Veterans Affairs Health Care System, Decatur, GA, United States

^e Institute of Biomedical Sciences, Faculty of Medicine and Faculty of Life Sciences, Universidad Andres Bello, Santiago, Chile

ARTICLE INFO

Keywords:

Vascular smooth muscle cell
Vasculature
ClpP
ClpXP complex
Mitochondria
Metabolism
NAD⁺
Sirtuin 1
VSMC
TIC10
Aneurysms

ABSTRACT

Vascular smooth muscle cells (VSMCs), known for their remarkable lifelong phenotypic plasticity, play a pivotal role in vascular pathologies through their ability to transition between different phenotypes. Our group discovered that the deficiency of the mitochondrial protein Poldip2 induces VSMC differentiation both in vivo and in vitro. Further comprehensive biochemical investigations revealed Poldip2's specific interaction with the mitochondrial ATPase caseinolytic protease chaperone subunit X (CLPX), which is the regulatory subunit for the caseinolytic protease proteolytic subunit (ClpP) that forms part of the ClpXP complex – a proteasome-like protease evolutionarily conserved from bacteria to humans. This interaction limits the protease's activity, and reduced Poldip2 levels lead to ClpXP complex activation. This finding prompted the hypothesis that ClpXP complex activity within the mitochondria may regulate the VSMC phenotype.

Employing gain-of-function and loss-of-function strategies, we demonstrated that ClpXP activity significantly influences the VSMC phenotype. Notably, both genetic and pharmacological activation of ClpXP inhibits VSMC plasticity and fosters a quiescent, differentiated, and anti-inflammatory VSMC phenotype. The pharmacological activation of ClpP using TIC10, currently in phase III clinical trials for cancer, successfully replicates this phenotype both in vitro and in vivo and markedly reduces aneurysm development in a mouse model of elastase-induced aortic aneurysms. Our mechanistic exploration indicates that ClpP activation regulates the VSMC phenotype by modifying the cellular NAD⁺/NADH ratio and activating Sirtuin 1. Our findings reveal the crucial role of mitochondrial proteostasis in the regulation of the VSMC phenotype and propose the ClpP protease as a novel, actionable target for manipulating the VSMC phenotype.

1. Introduction

Vascular smooth muscle cells (VSMCs) play a critical role in maintaining vascular integrity and function. Differentiated VSMCs are characterized by the expression of proteins from the contractile apparatus, such as Myosin Heavy Chain (MYH11), Transgelin (TAGLN), Calponin 1 (CNN1), and Alpha Smooth Muscle Actin (ACTA2) [1]. In addition, establishing and maintaining the VSMC differentiated phenotype requires the repression of the Krüppel-like zinc finger factor 4 (KLF4) [2], which antagonizes SMC-specific gene expression through various

mechanisms [3–5].

A unique characteristic of VSMCs is their remarkable plasticity throughout life, as they are not terminally differentiated. In response to various stimuli, such as cholesterol, growth factors, or mechanical injury, VSMCs dedifferentiate to adopt alternative phenotypes [1]. This ability is critical for vessel maturation, remodeling, and injury repair but also increases susceptibility to vascular diseases [1]. For instance, in aortic aneurysms, weakening of arterial walls results from complex vessel wall remodeling, where VSMC phenotypic modulation plays a central role [6–15].

* Corresponding author. Biomedical Sciences, Faculty of Medicine and Faculty of Life Sciences, Universidad Andres Bello, Santiago, Chile.
E-mail address: asanmartin@emory.edu (A. San Martin).

<https://doi.org/10.1016/j.redox.2024.103203>

Received 19 February 2024; Received in revised form 12 May 2024; Accepted 20 May 2024

Available online 21 May 2024

2213-2317/© 2024 Published by Elsevier B.V. This is an open access article under the CC BY-NC-ND license (<http://creativecommons.org/licenses/by-nc-nd/4.0/>).

Our laboratory's recent work highlighted the crucial role of mitochondria and metabolic signaling in controlling the VSMC phenotype [16]. Initially, we focused on a previously uncharacterized mitochondrial protein called Poldip2. Our findings revealed that Poldip2 deficiency promotes the differentiation of VSMCs and limits their phenotypic plasticity, both in vitro and in vivo [16]. Our biochemical studies demonstrated that Poldip2 specifically binds to the Caseinolytic Mitochondrial Matrix Peptidase Chaperone Subunit X (CLPX) [17]. This is significant because CLPX is a key regulatory ATPase for the Caseinolytic Mitochondrial Matrix Peptidase Proteolytic Subunit (ClpP), a highly conserved serine protease [18]. Together, CLPX and ClpP form the ClpXP complex that participates in mitochondrial proteostasis [18].

In this molecular partnership, Poldip2 effectively sequesters CLPX, leading to the inactivation of ClpP [17]. Conversely, when Poldip2 levels are reduced, CLPX becomes available to activate ClpP, which then degrades its target proteins [17]. As previously mentioned, these Poldip2-deficient VSMCs also exhibit a remarkable degree of differentiation [16]. This relationship between Poldip2 deficiency, ClpP activation, and VSMC differentiation led us to hypothesize that ClpP activation directly regulates the VSMC phenotype.

In this paper, we report a novel role for the ClpXP complex, in that the activation of ClpP proteolytic activity induces a differentiated and anti-inflammatory phenotype in VSMCs, dependent on the increased cellular NAD⁺/NADH ratio and the activation of the NAD⁺-dependent deacetylase Sirtuin 1 (SIRT1).

ClpP agonists are the subject of active investigation for cancer treatment. One such ClpP agonist is TIC10 (ONC201) [19], which is currently in Phase III clinical trials for glioma treatment. Interestingly, in our study, TIC10 mimics the ClpXP gain-of-function VSMC differentiated phenotype and effectively reduces the aorta diameter in a mouse model of elastase-induced aneurysm formation. Together, these findings suggest that the mitochondrial protease ClpP, a druggable target, plays a critical role in regulating VSMC phenotype. Our study reveals a novel regulatory mechanism in VSMC biology. Understanding this mechanism opens new avenues for exploring how VSMCs transition between different phenotypes and how this transition might be manipulated for therapeutic purposes.

2. Methods

2.1. General reagents

Nicotinamide Ribose, ADEP1, and TIC10/ONC201 were obtained from Cayman Chemical. Recombinant human platelet-derived growth factor (PDGF)-BB was obtained from R&D Systems Inc.

2.2. Elastase model of aneurysm

We used the elastase-induced model of aneurysm formation in mice as previously described [20,21]. Briefly, 10-week wild-type C57BL/6 J male mice (Jackson Laboratory) were allowed to acclimate in-house for two weeks. Male mice were injected with TIC10 (50 mg/kg) or vehicle on days -6, -1, 4, and 9 via IP. On the day of the surgery, general anesthesia was achieved by isoflurane (3 % in O₂) inhalation. Next, the infrarenal abdominal aorta was exposed for 10 min to soaked cotton with 5 µL of type I porcine pancreatic elastase (0.45 U/mL, Sigma). Mice were euthanized by CO₂ asphyxiation, and infrarenal abdominal aortas from both groups were harvested for tissue analysis on day 14.

Additionally, abdominal aortas (infrarenal segment) were visualized in anesthetized mice at baseline and on days 7 and 14 after surgery using a portable Vevo 3100 Micro-Imaging System with a D550 probe (Fuji).

Longitudinal and cross-sectional images of the abdominal aortas were captured and normal and maximal diameters of the abdominal aortas at aneurysm sites were measured. All recordings were made in a blinded manner.

2.3. Cell culture

Primary Human Aortic Smooth Muscle Cells (HASMCs) were obtained from human aortic tissues and cryopreserved at passage 3 (ThermoFisher Scientific, #C0075C). For this study, cell cultures originating from a single donor were used, although cells from multiple donors were employed throughout the research. Culturing of HASMCs adhered to the protocol recommended by the supplier, utilizing basal media 231 enhanced with specific growth supplements.

2.4. Cell transfection and viral expression of CLPX

Cells were transfected using Lipofectamine RNAiMAX reagent (Thermo-Fisher) following the manufacturer's suggested protocol. Sequences were: For CLPX: 5'-CAGAUUGGCACUAGAACGA[dT][dT]; for CLPP 5'-GCUCAAGAAGCAGCUCUAU[dT][dT]. For SIRT1:5'-GUGUCAUGGUUCCUUUGCA[dT][dT]. In all experiments, AllStars Negative Control siRNA (Qiagen cat#1027281) was used as a control siRNA. Cells were harvest 48 h after transfection.

Adenovirus with CMV promoter-driven expression of the human Caseinolytic Mitochondrial Matrix Peptidase Chaperone Subunit X (ClpX) cDNA (Accession NM_006660) in pAD vector with kanamycin selection and C-terminal FLAG and His tags were obtained from Vigene Bioscience (catalog# VH847033). Control Adenovirus was also from Vigene (catalog# CV10001).

The Emory Environmental Health and Safety Office approved the use of recombinant nucleotides and adenoviruses.

2.5. Immunohistochemistry and Verhoeff Van Gieson (VVG) elastic staining

Aortic sections were deparaffinized, rehydrated, and then blocked for 1 h at room temperature (2 % BSA and 5 % donkey serum in Universal buffer). Next, sections were incubated with ACTA2 antibody (Sigma Aldrich A2547, 1:400) for 1 h at 4 °C. Then incubated with Alexa Fluor® 647-AffiniPure donkey Anti-mouse IgG (Jackson ImmunoResearch Cat# 715-605-150) and counterstained with DAPI. Sections treated with secondary antibodies alone did not show specific staining. Confocal micrographs were acquired with a Zeiss LSM 800 Confocal Laser Scanning Microscope using a 63× oil objective lens and Zeiss ZEN acquisition software. When comparing sections from different experimental groups, all confocal microscope image threshold settings remained constant.

Elastin staining was performed using a commercial kit (Sigma Aldrich, HT25A), following the manufacturer's recommendations. Images were captured using the Hamamatsu NanoZoomer SQ Whole Slide Scanner, specifically designed for Brightfield imaging. To evaluate the structural integrity of elastin within the medial layer, we utilized Image J software (National Institutes of Health, Bethesda, MD, USA) with the color threshold tool. The outer boundary of the medial layer was identified at the point where disrupted or concentric elastin rings transitioned to the connective tissue of the adventitial layer.

2.6. Western blots

Total protein lysates were prepared in RIPA buffer with Glycerol (Tris-HCL 100 mM, NaCL 300 mM, Triton x 100 2 %, Sodium deoxycholate 1 %, SDS 0.2 % and Glycerol 10 %). Protein samples were separated on Express-Plus Page Gels (GenScript) with Tris-MOPS buffer containing SDS and transferred onto Immobilon-P membrane (Millipore, IPVH00010). All antibodies were incubated for 24 h at 4 °C. Protein bands were visualized using HRP-conjugated secondary antibodies and ECL Western Blotting Substrate (Luminata Crescendo, Millipore) and imaged on a Kodak Camera System.

2.7. Western blotting of aortic tissue

Mouse aortas were harvested, cleaned of fat and connective tissue, and then flash-frozen in liquid nitrogen. Frozen aortas were ground into a fine powder using a pre-chilled mortar and pestle. Proteins were extracted in RIPA buffer (25 mmol/L HEPES, 150 mmol/L KCl, 1.5 mmol/L MgCl₂, 1 mmol/L EGTA, 10 mmol/L Na-pyrophosphate, 10 mmol/L NaF, 1 % Na deoxycholate, 1 % Triton X 100, 0.1 % SDS, 10 % Glycerol, Na-orthovanadate, and protease inhibitors) from their lysates, sonicated, and cleared at 14,000×g for 20 min. Proteins were separated using SDS-PAGE and transferred to Immobilon-P polyvinylidene difluoride (PVDF) membranes (Millipore), blocked with 5 % non-fat dairy milk, and incubated with primary antibodies. List of antibodies can be found in [Table 1](#).

2.8. Assessment of bioenergetics

HASMCs were plated (20,000 cells/well) on Seahorse Extracellular Analyzer XF96 plates in culture media, and after 24hrs, cells were treated with TIC10 or ADEP1 or were transfected or infected with the corresponding siRNA or expression virus. Measurements of the oxygen consumption rate (OCR) and extracellular acidification rate (ECAR) were measured as previously described [22] by the XF96e extracellular flux analyzer (Agilent-Seahorse XF technology). After completion of the experiments, the total protein in each well was determined by the BCA protein assay (BioRad) for data normalization.

2.9. SIRT1 enzymatic activity assay

SIRT1 activity was measured using a fluorometric SIRT1 Activity Assay Kit (Abcam #ab156065) as previously described [23]. Briefly, cells were seeded into 6 well plates (2×10^5 cells/well). The day after, the medium was removed, and cells were treated with TIC10 or ADEP1 or were transfected or infected with the corresponding siRNA or expression virus. After 48hrs, cells were harvested in the recommended lysis buffer. Reactions were initiated by adding cell lysates to the reaction mixture containing SIRT1 assay buffer, fluoro-substrate peptides (100 mM), and NAD⁺ (100 mM). Fluorescence intensity was measured for 30 min at 2–3 min intervals on a microplate fluorometer (excitation, 350 nm; emission, 460 nm). SIRT1 activity was calculated within the linear range of reaction velocity and normalized against the protein concentration in WT control cells.

Table 1
Antibodies used in this study.

Protein	Company	Catalog number
PAN-ACTIN	Santa Cruz	sc-1615
PAN-ACTIN	Cell Signaling	8456S
SDHA	Cell Signaling	5839S
UQCRC2	GeneTex	GTX114873
CLPX	Abcam	ab168338
CLPX	GeneTex	GTX53477
CLPP	Cell Signaling	14181S
VCAM1	Abcam	ab123801
CNN	Santa Cruz	SC-136987
TAGLN	Abcam	ab14106
ACTA2	Sigma	A5228
SIRT1	Cell Signaling	8469S
MYOCD	R&D Systems	MAB4828
MRTFA	Novus	NBP1-88498
KLF4	R&D Systems	AF3640
CD68	Cell Signaling	86985S
LGALS3	Cell Signaling	12733S
CCL2	BD Biosciences	551217
ICAM	Thermo Fisher	MA5407
SIRT1	Cell Signaling	9475S

2.10. NAD⁺ and NADH quantification

NAD⁺ and NADH concentrations were measured using the NAD⁺/NADH-Glo™ assay (Promega #G9071) following the manufacturer's instructions.

2.11. Statistical analysis

Images that better represent the data set averages were selected as representative. Data are presented as mean ± SEM from a minimum of 4 independent experiments (biological replicates). For variables that passed the Shapiro-Wilk normality test, significance was determined using a *t*-test for unpaired samples, 1-way ANOVA, or 2-way ANOVA, followed by Dunnett's or Tukey's post-hoc test for multiple comparisons. Non-parametric variables and ranks were compared using the Mann-Whitney test or the Kruskal-Wallis test. The GraphPad Prism 10.0.2 software was used for statistical analysis. A threshold of *P* < 0.05 was considered significant and is indicated by * for *P* < 0.05, ** for *P* < 0.01, *** for *P* < 0.001, and **** for *P* < 0.0001.

3. Results

To investigate a possible relationship between the ClpXP protease complex and the VSMC phenotype, we employed gain- and loss-of-function approaches. As anticipated, the reduction in either component of the ClpXP complex, ClpP or CLPX, led to a notable decline in protease activity, evident by the accumulation of recognized substrates of ClpP: the succinyl CoA dehydrogenase subunit A (SDHA) [24] and the Ubiquinol-Cytochrome C Reductase Core Protein 2 (UQCRC2) [25] ([Fig. 1](#)).

The downregulation of ClpP or CLPX markedly alters the expression profile of vascular smooth muscle cell (VSMC) phenotypic markers. This modulation triggers a significant reduction in the levels of VSMC differentiation proteins, including ACTA2, TAGLN, and CNN, alongside an upsurge in KLF4 expression, as illustrated in [Fig. 1](#). Furthermore, ClpXP loss-of-function-induced VSMC dedifferentiation was accompanied by an increase in the inflammatory cytokines Vascular Cell Adhesion Protein 1 (VCAM1), Intercellular Adhesion Molecule 1 (ICAM1), and C-C motif Chemokine Ligand 2 (CCL2), and the expression of the transitional marker Galactin 3 (LGALS3) [26–28] ([Fig. 1](#)).

Overexpression of the ATPase chaperone CLPX is sufficient to cause the activation of ClpP in prokaryotes and eukaryotes [29,30]. Thus, we used this approach to investigate the effects of ClpXP-gain-of-function. As shown in [Fig. 2](#), forced expression of CLPX was sufficient to activate the ClpX complex, inducing the degradation of SDHA and UQCRC2—while concurrently increasing the expression of differentiation markers in VSMCs under basal and platelet-derived growth factor (PDGF)-stimulated conditions ([Fig. 2](#)). Furthermore, in addition to increased differentiation and reduced plasticity, ClpP activation inhibited the expression of inflammatory cytokines, a phenomenon particularly evident in cells subjected to PDGF stimulation ([Fig. 2](#)). These experiments demonstrated that the expression and activity of the ClpXP proteolytic complex in the mitochondria has a remarkable capacity to regulate the VSMC phenotype, inducing a differentiated, non-inflammatory phenotype. Consequently, our research efforts focused on understanding the mechanism by which ClpP activation drives differentiation in VSMCs.

Building on our prior studies that underscore the impact of ClpP activation on VSMC metabolism [17] and considering its capability to degrade critical constituents of the electron transfer chain, such as SDHA and UQCRC2 ([Fig. 2](#)), the observation that activating ClpP by overexpressing CLPX leads to reduced basal mitochondrial respiration and ATP production linked to respiration (detailed in [Fig. 3A](#) and [B](#)) was anticipated. Despite the inhibition of mitochondrial respiration when ClpP is activated, the energy phenotype revealed that CLPX overexpressing cells did not upregulate glycolysis and transitioned into a

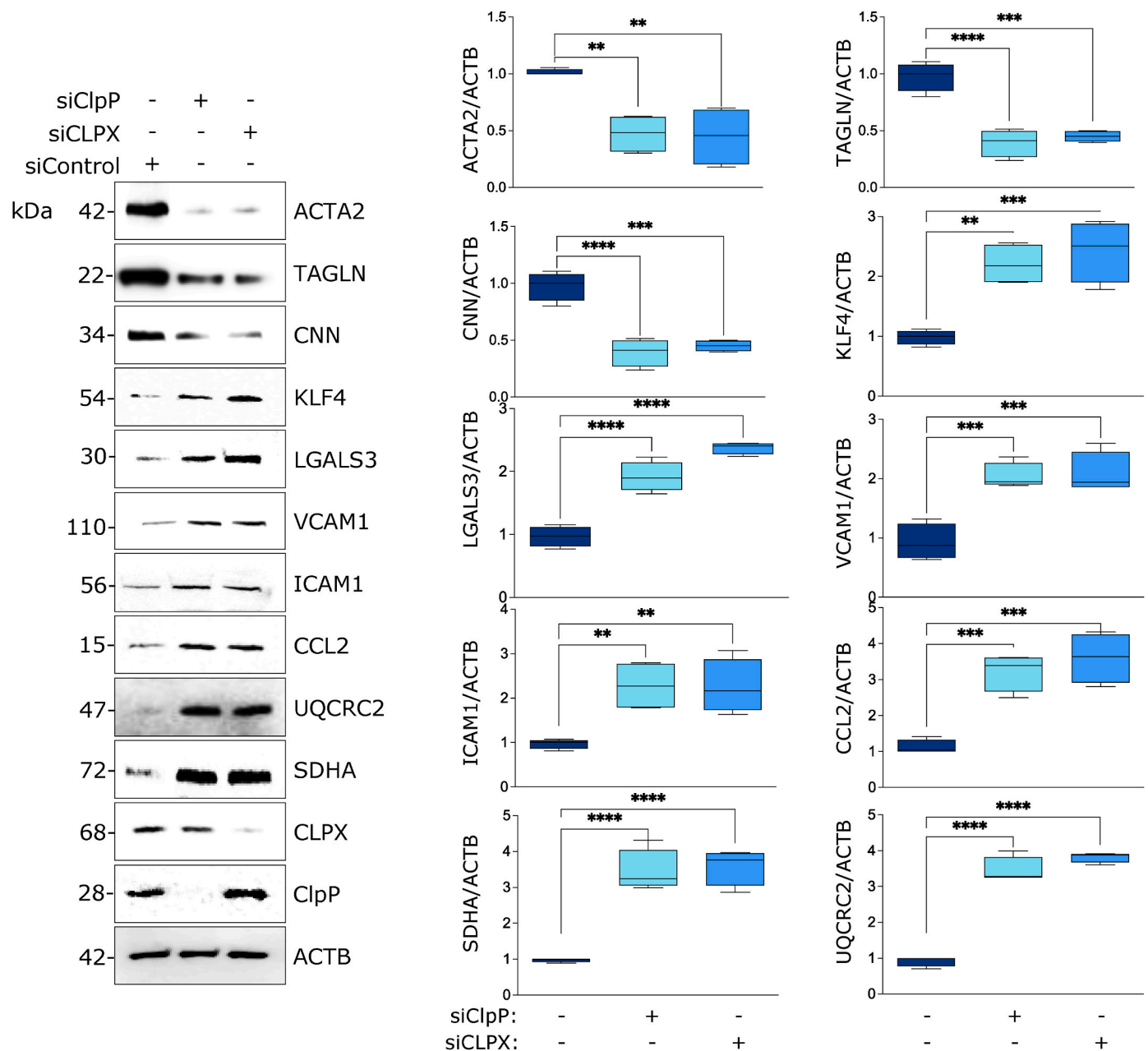


Fig. 1. ClpXP loss-of-function reduces differentiation and increases inflammatory cytokines expression in VSMCs. Representative western blots of protein expressed in HASMCs transfected with siRNA control or against CLPX or siClpP (left). Box-and-whisker plots illustrate the distribution of protein expression levels across multiple experiments (right). The box represents the interquartile range, encompassing the 25th to 75th percentiles of the dataset, with the median protein expression level indicated by a line within the box. Whiskers extend to the 5th and 95th percentiles, denoting the range of data of 4–5 independent experiments. A threshold of $P < 0.05$ was considered significant and is indicated by * for $P < 0.05$, ** for $P < 0.01$, *** for $P < 0.001$, and **** for $P < 0.0001$.

quiescent state (Fig. 3C). Regarding total cellular levels of nicotinamide adenine dinucleotide in its oxidized (NAD^+) and reduced ($NADH$) forms, we found that the activation of ClpP leads to elevated NAD^+ levels while simultaneously lessening $NADH$ content within the cell (Fig. 3D), resulting in a marked enhancement of the $NAD^+/NADH$ ratio (Fig. 3E).

The association between heightened $NAD^+/NADH$ ratios and Sirtuin (SIRT)1 activation in other cell types [31] led us to examine whether ClpXP-gain-of-function activates SIRT1. Consistent with this previous report, we observed that the metabolic changes observed were coupled with a notable upsurge in SIRT1 activity (Fig. 4A). SIRT1 is a NAD -dependent protein deacetylase linked to preserving the VSMC's contractile phenotype [32], and polymorphisms on its promoter region have been associated with cardiovascular diseases [33,34]. With this in

mind, we tested whether SIRT1 was involved in the VSMC phenotypic regulation downstream of ClpXP activation. We confirmed that SIRT1 expression is required for the VSMC phenotypic regulation induced by ClpXP activation (Fig. 4B and C). These cumulative findings illustrate that ClpXP gain-of-function initiates a metabolic adaptation, leading to a metabolically quiescent phenotype characterized by an upregulated $NAD^+/NADH$ ratio and SIRT1 induction. This, in turn, mediates the establishment of a differentiated and anti-inflammatory phenotype in VSMCs following ClpP activation.

To investigate the translational potential of pharmacological activation of ClpP, we utilized two drugs known to activate ClpP: a naturally occurring antibiotic, the acyldepsipeptide ADEP1 [35,36], and the synthetic imipridone TIC10 [19]. So, we tested the ability of these drugs

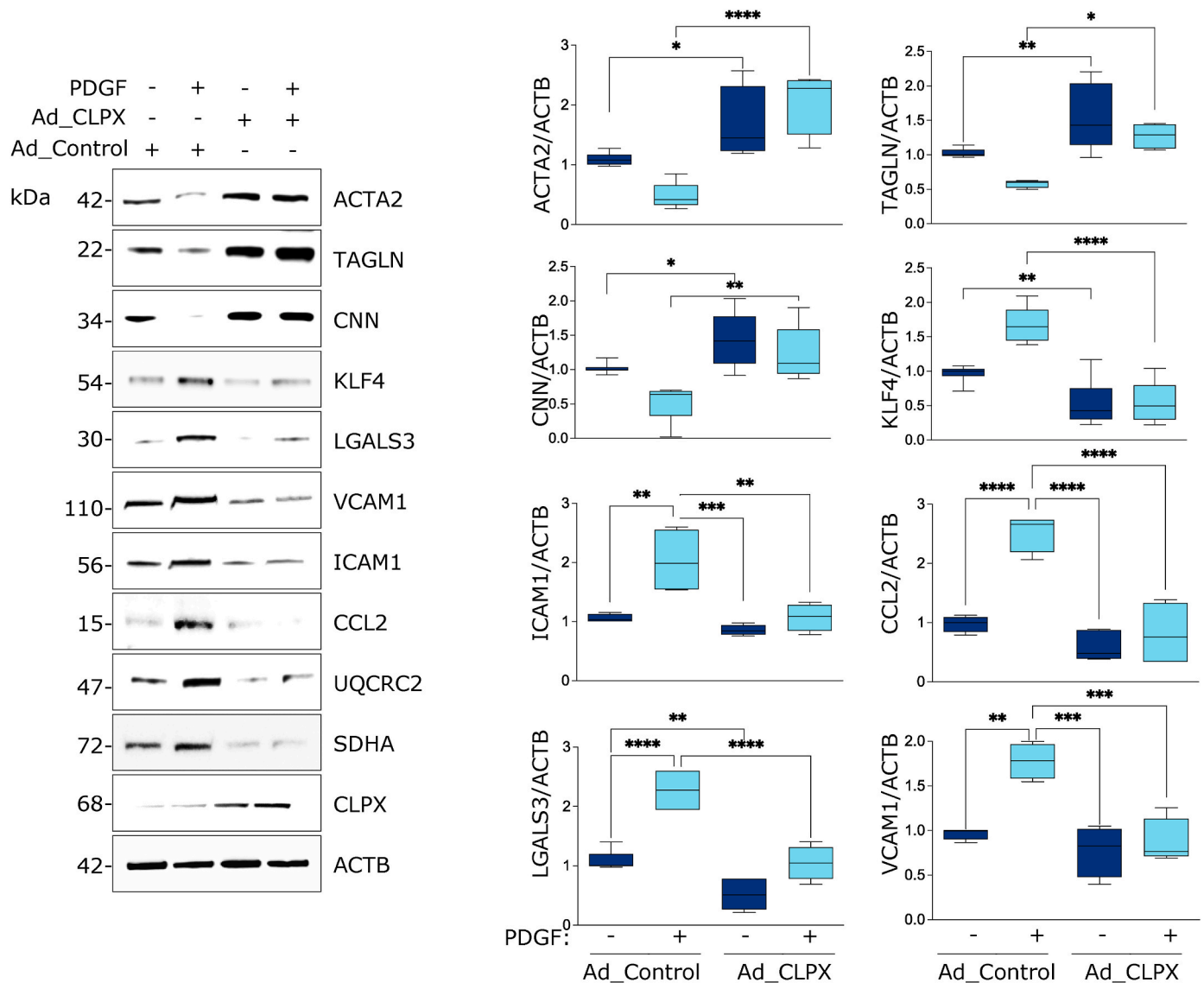


Fig. 2. ClpXP gain-of-function induces differentiation and increases inflammatory cytokines expression in VSMCs. Representative western blots showing protein expression in human aortic smooth muscle cells (HASMCs) transduced with either an adenovirus expressing CLPX or a control adenovirus containing no insert (left). Cells were treated with either platelet-derived growth factor (PDGF) at a concentration of 10 ng/mL or a vehicle control for 48 h. Box-and-whisker plots illustrate the distribution of protein expression levels across multiple experiments (right). The box represents the interquartile range, encompassing the 25th to 75th percentiles of the dataset, with the median protein expression level indicated by a line within the box. Whiskers extend to the 5th and 95th percentiles, denoting the range of data of 5–6 independent experiments. A threshold of $P < 0.05$ was considered significant and is indicated by * for $P < 0.05$, ** for $P < 0.01$, *** for $P < 0.001$, and **** for $P < 0.0001$.

to induce the ClpP-mediated phenotypic regulation in VSMCs. Both drugs induced the degradation of SDHA and UQCRC2, evidence of their ability of activating ClpP (Fig. 5). As expected, the treatment with these drugs reiterates the effect of ClpXP-gain-of-function on VSMC phenotype (Fig. 5). Furthermore, these drugs also recapitulate key elements of the mechanism as they increased the NAD^+ and NAD^+/NADH ratio (Supplemental Fig. 1A) and SIRT1 activation (Supplemental Fig. 1B). Similarly, pharmacological activation of ClpP-induced VSMC phenotypic regulation occurs by a SIRT1-dependent mechanism (Supplemental Fig. 2).

TIC10, an orally bioavailable small molecule, is currently in Phase III clinical trials for the treatment of glioma (clinicaltrials.gov ID: NCT05580562 and NCT05476939). Consequently, we were particularly interested in testing its ability to control VSMC phenotype in vivo as proof of concept for potentially repurposing this drug to treat vascular diseases involving VSMC phenotypic modulation. We discovered that two 50 mg/kg injections can modulate the VSMC phenotype and

inflammatory cytokine expression in the aorta of male mice (Supplemental Figure 3), closely mirroring our in vitro data (Fig. 5). We confirmed that this effect is mediated by ClpP, as the absence of ClpP nullifies TIC10's effects on the VSMC phenotype (Supplemental Figure 4). Collectively, these findings strongly suggest that TIC10 induces a differentiated phenotype in VSMCs both in vitro and in vivo primarily through the activation of ClpP.

Aortic aneurysms are a life-threatening disease currently lacking effective pharmacological treatments. Given the central role of VSMC phenotypic modulation in this disease [8,9], we investigated the efficacy of TIC10 in preventing aneurysm formation using an elastase-induced mouse model [20,21]. Male mice received intraperitoneal injections of either TIC10 (50 mg/kg) or a control vehicle, administered both before and after surgery, as depicted in Fig. 6A. TIC10 treatment markedly decreased the aortic diameter (Fig. 6B) and limited maximal aortic dilation (Fig. 6C) when compared to control mice. Observing the pronounced difference in aneurysm development between the

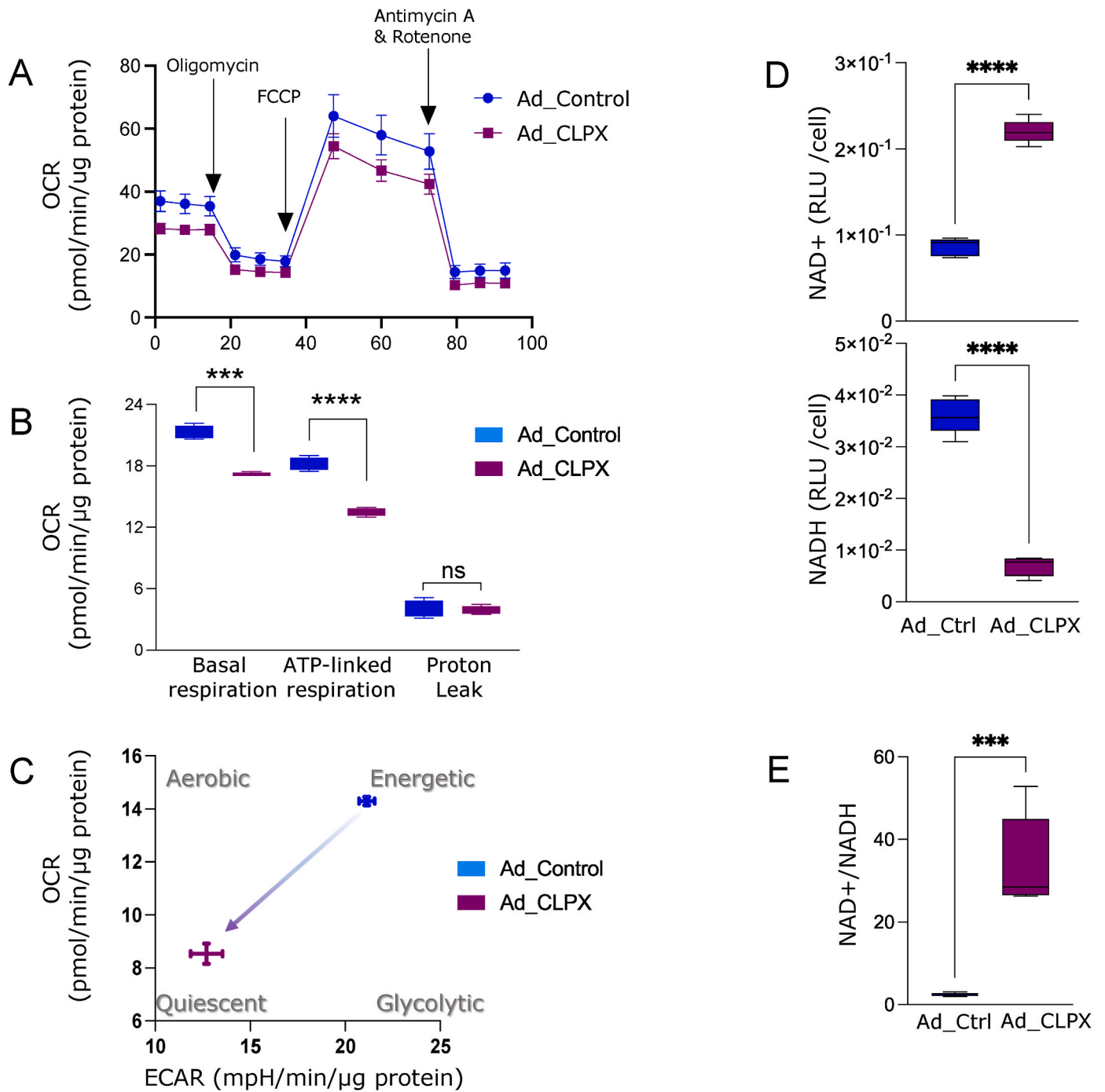


Fig. 3. Metabolic changes induced by ClpXP gain-of-function in VSMCs. (A) Profile of mitochondrial respiration over time in HASMCs expressing Ad_Control or Ad_CLPX. Basal OCR measurements were made, and 1 $\mu\text{g}/\text{mL}$ oligomycin, 1 μM carbonyl cyanide-4-(trifluoromethoxy)phenylhydrazone (FCCP), and 10 μM antimycin-A and 1 μM rotenone were then sequentially injected. Data are presented as mean \pm SE (B) Box-and-whisker plots from the data obtained from the analysis of OCR profiles (basal corresponds to antimycin-A-inhibitable and ATP-linked corresponds to oligomycin-inhibitable). (C) Energy map showing the metabolic reprogramming (D) Box-and-whisker plots depicting total cellular NAD^+ and NADH levels and (E) Box-and-whisker plots depicting NAD^+/NADH ratio induced by ClpXP gain-of-function in VSMCs. Box-and-whisker plots illustrate the distribution of protein expression levels across multiple experiments (right). The box represents the interquartile range, encompassing the 25th to 75th percentiles of the dataset, with the median protein expression level indicated by a line within the box. Whiskers extend to the 5th and 95th percentiles, denoting the range of data of 4–5 independent experiments. A threshold of $P < 0.05$ was considered significant and is indicated by * for $P < 0.05$, ** for $P < 0.01$, *** for $P < 0.001$, and **** for $P < 0.0001$.

TIC10-treated and control groups, we further evaluated elastin degradation and ACTA2 expression at the 14-day mark. Utilizing Verhoeff–Van Gieson (VVG) staining and indirect immunofluorescence, we found that elastin preservation was notably better in the TIC10 group (Supplementary Figure 5A). ACTA2 staining was significantly more pronounced in the TIC10-treated mice compared to the controls

(Supplementary Figure 5B). Together, these results underscore the potential of targeting ClpP as a strategic approach to enhance VSMC differentiation in vivo. Moreover, they demonstrate the effectiveness of TIC10 in reinforcing the structural integrity of vessel walls and effectively slowing down the progression of aneurysms in this experimental model.

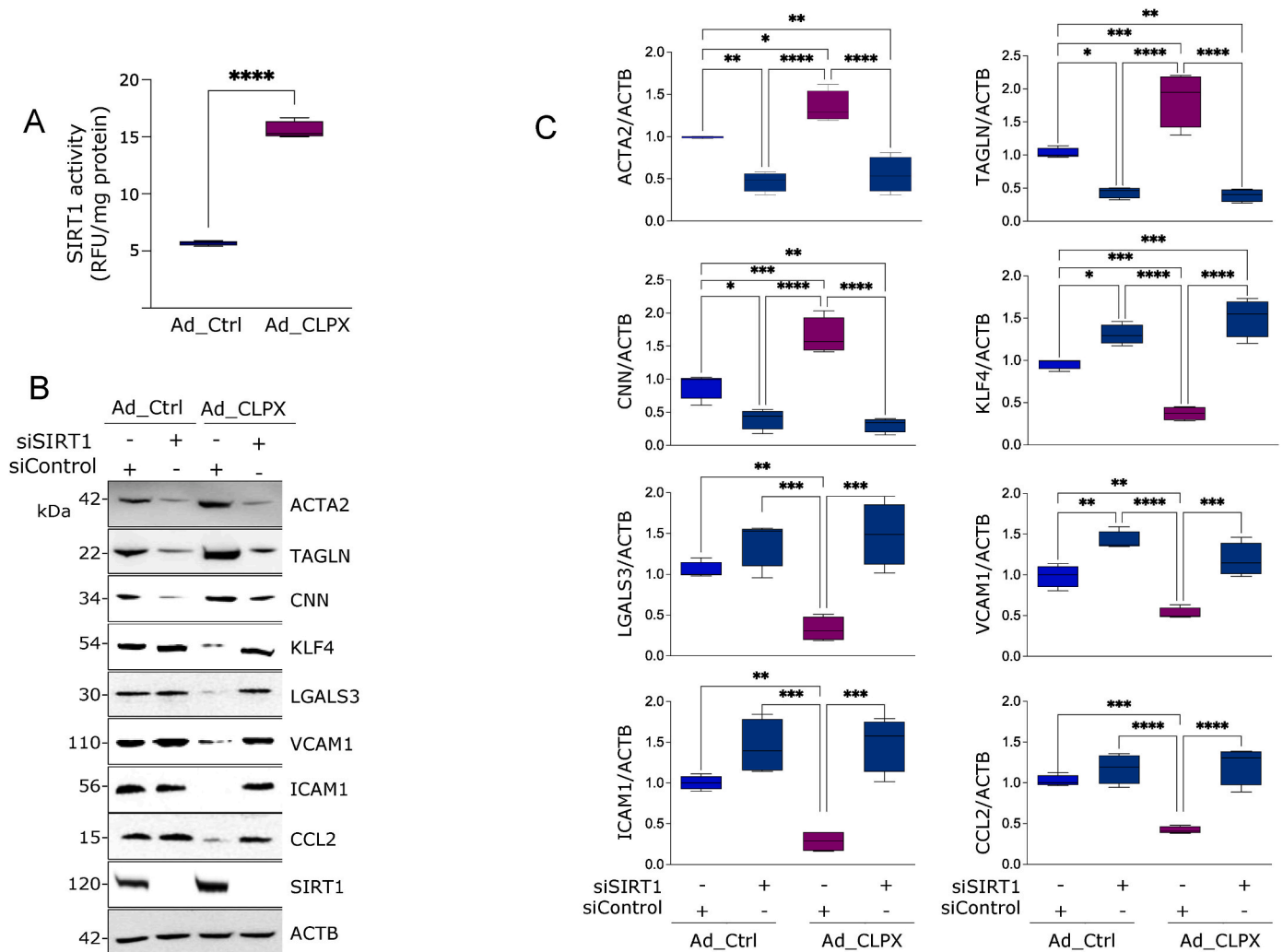


Fig. 4. ClpXP-induced VSMC phenotypic modulation is mediated by SIRT1 activation in VSMCs. (A) Human aortic smooth muscle cells (HASMCs) were transduced with either an adenovirus expressing CLPX or a control adenovirus containing no insert and SIRT1 activity was measured as described in the methods section. (B) Representative western blots of protein expression in HASMCs transduced with either an adenovirus expressing CLPX or a control adenovirus containing no insert in cells transfected with control siRNA or SIRT1 directed siRNA. (C) Box-and-whisker plots depicting NAD^+/NADH ratio induced by ClpXP gain-of-function in VSMCs. Box-and-whisker plots illustrate the distribution of protein expression levels across multiple experiments. The box represents the interquartile range, encompassing the 25th to 75th percentiles of the dataset, with the median protein expression level indicated by a line within the box. Whiskers extend to the 5th and 95th percentiles, denoting the range of data of 4–5 independent experiments. A threshold of $P < 0.05$ was considered significant and is indicated by * for $P < 0.05$, ** for $P < 0.01$, *** for $P < 0.001$, and **** for $P < 0.0001$.

4. Discussion

Maintaining proteostasis is critical for normal cell development and the stress response to environmental factors and pathogens [37,38]. Cellular dysregulation of proteostasis is linked to aging-associated cellular senescence [38,39] and several human diseases such as Alzheimer's, Parkinson's, Huntington's, and Creutzfeldt-Jacob diseases [40].

Moving beyond general proteostasis, we delve into the specific role of ClpP, which is highly conserved in prokaryotes and the mitochondria and plastids of eukaryotes [18], highlighting its biological importance.

In humans, the conformation and activity of the mitochondrial protease ClpP are regulated by its association with the chaperone CLPX [41]. Our previous research found that Poldip2 specifically binds to CLPX to negatively regulate ClpP activity [17]. The interaction of Poldip2 and CLPX has been subsequently validated across various systems [42,43]. The fact that ClpP activation induces differentiation in VSMC (Figs. 2 and 6) is consistent with the observation that low Poldip2 induces a similar differentiated phenotype [16].

Turning our attention to metabolic aspects, we observed shifts in the NAD^+/NADH ratio. Although an increase in NAD^+ has been documented following targeted depletion of SDHA [44] and SDHB [45], it was somewhat surprising to discover that ClpXP activation elevates the NAD^+/NADH ratio. One might intuitively assume that disrupting the electron transport chain would reduce the NAD^+/NADH ratio due to respiratory complex I's hindered ability to oxidize NADH. This would be the case unless the NADH oxidation process remains unaffected by ClpXP upregulation. The mammalian respiratory complex I is a distinct L-shaped structure, composed of a transmembrane P-module functioning as the proton pump, an adjacent ubiquinone-reducing-Q-module, and a matrix NADH-oxidizing-N-module [46]. Intriguingly, recent findings suggest that ClpXP consistently oversees the high turnover rate of the NADH-oxidizing N-module, independent of the entire complex [47]. Therefore, the fleeting half-life of the N-module subunits might render them resistant to augmented ClpXP activity, ensuring that the NADH oxidizing function of Complex I remains intact. Moreover, as the cell transitions to a quiescent state, it utilizes less NAD^+ for oxidative catabolic reactions, leading to an accumulation of NAD^+ and a consequent increase in the NAD^+/NADH

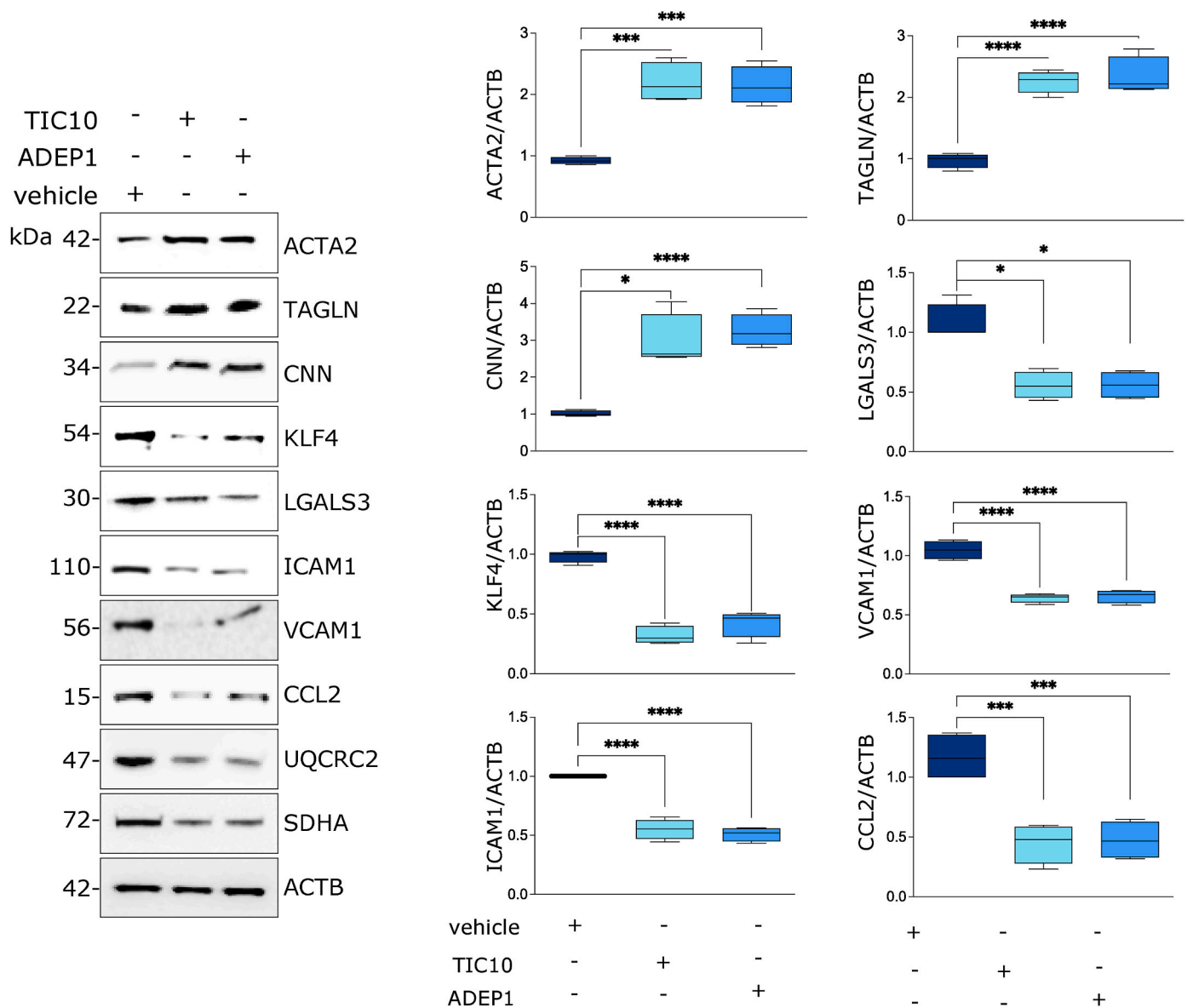


Fig. 5. Pharmacological activation of ClpP induces a differentiated and anti-inflammatory phenotype in VSMCs. Representative western blots of protein expression in human aortic smooth muscle cells treated with TIC10 (1 μ M) or ADEP1 (1 μ M) for 48 h (right). Box-and-whisker plots illustrate the distribution of protein expression levels across multiple experiments (right). The box represents the interquartile range, encompassing the 25th to 75th percentiles of the dataset, with the median protein expression level indicated by a line within the box. Whiskers extend to the 5th and 95th percentiles, denoting the range of data of 5–6 independent experiments. A threshold of $P < 0.05$ was considered significant and is indicated by * for $P < 0.05$, ** for $P < 0.01$, *** for $P < 0.001$, and **** for $P < 0.0001$.

ratio. Further investigations are crucial to comprehend how specific shifts in mitochondrial proteostasis result in such pronounced functional changes.

Aneurysms are pathological enlargements of the diameter of an arterial wall that become vulnerable to pressure; continued weakening leads to rupture and hemorrhage. Aortic aneurysms constitute a life-threatening disease without an effective pharmacological treatment. Aortic aneurysm pathophysiology is complex and involves active vessel wall remodeling in which VSMC phenotypic modulation and dedifferentiation plays a central role [8,9].

In human and rodent studies, VSMC phenotypic modulation has been reported in abdominal aortic aneurysms (AAA) [48–60] and thoracic aorta aneurysms (TAA) [61–68]. Furthermore, in animal models of aortic aneurysms, SMC-specific gene downregulation precedes the weakening of the arterial wall [69] and KLF4 deficiency inhibits aneurysm formation [60]. Additionally, heterozygous mutations, or differential expression of proteins from the VSMC contractile apparatus, as

well as the kinases that regulate their assembly, have been linked to the formation of aneurysms in humans [6,7,10–15].

To validate our findings regarding the role of ClpP activation in maintaining a highly differentiated VSMC phenotype *in vivo*, we utilized an elastase-induced aneurysm model in animals. Our observations indicate that TIC10 treatment effectively inhibits aneurysm formation in this model. The aneurysm formation inhibition observed in our study is similar to that reported in animals with VSMC-specific deficiency of KLF4, which inhibits VSMC phenotypic modulation [60]. While these results are consistent with the preservation of the VSMC phenotype, it's important to note that we cannot completely rule out the potential involvement of TIC10-mediated ClpXP activation in other cell types within this mechanism.

These drugs bind to each monomer of ClpP via non-covalent allosteric interactions, rendering a conformational change that opens the proteolytic chamber, activating it without the chaperone CLPX [36].

Recently, it was shown that ClpP is the molecular target of the small

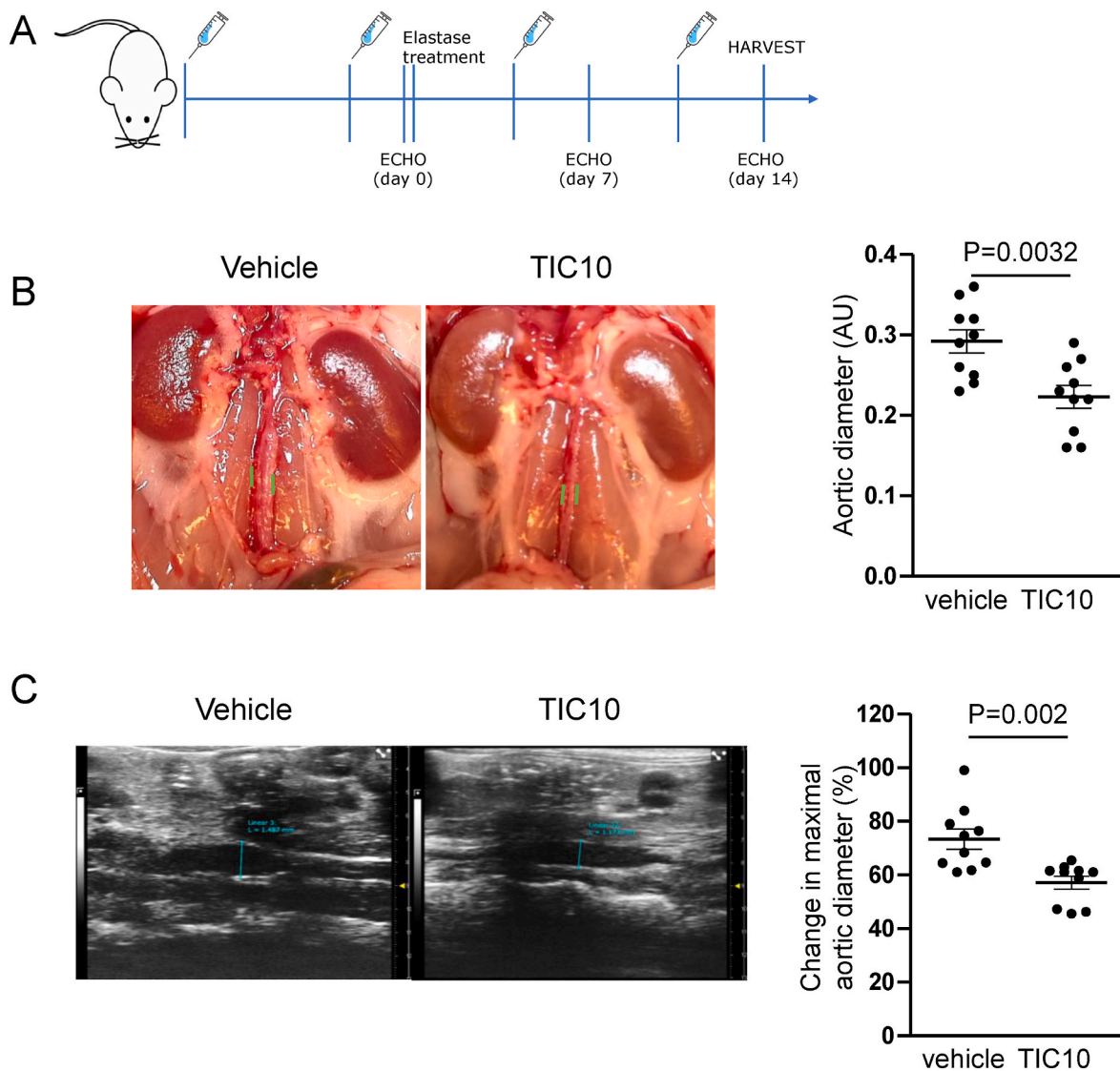


Fig. 6. TIC10 treatment results in attenuated aneurysm formation. (A) Model illustrating the timeline of the experiment, TIC10 (50 mg/kg) injections, and differences in aortic diameters between baseline and at 14 days, quantified by ECHO. The recording and subsequent analysis were blinded to the treatment regimen assignment. (B) (Left) Representative images from the experimental animals in each group at day 14. (Right) Scatter dot plots illustrating the aortic diameter value for each experimental animal, with the median value indicated by a line. (C) (Left) Differences in aortic diameters between baseline and at 14 days were quantified by ECHO for the same experimental animal. Representative ECHO images are shown. The recording and subsequent analysis were blinded to the assignment of the treatment regimen. (Right) Scatter dot plots illustrate the value for the % of maximal aortic dilation at day 14 for each experimental animal, with the median value indicated by a line. Each experimental group was composed of 10 animals.

molecule TIC10 (ONC201) [19,41], currently in Phase III clinical trials for glioma treatment. Detailed biochemical and crytalography data shows that TIC10 binds to ClpP via non-covalent allosteric interactions, rendering a conformational change that opens the proteolytic chamber, activating it in the absence of the chaperone a CLPX chaperone-independent manner [19,36]. In our studies, we confirm that ClpP is the molecular target of TIC10 as it is required for this drug to induce the phenotypic changes in VSMCs (Supplementary Fig. 4).

Regarding the dosage of TIC10 used in our study, we initially relied on a substantial amount of published data [36,70–86]. Typical dosages for rodents reported in these studies range from 25 to 50 mg/kg, with the highest recorded dosage being 100 mg/kg [82]. Bearing this in mind, we conducted preliminary studies (data not shown) and concluded that the effect on VSMC phenotype was within the range of dosages previously used in animal research. Consequently, we decided to use a dosage of 50 mg/kg (Supplementary Figure 3).

Although there are several mouse models for aneurysm formation,

none fully encapsulate the complexities of human abdominal aortic aneurysms. However, we chose the elastase model due to its reliable replication of key pathophysiological features characteristic of human aneurysms, specifically its ability to induce aneurysms without causing dissections. Crucially, this model offers a high degree of reproducibility, consistently yielding aneurysms of similar sizes and at similar locations, making it particularly valuable for comparative studies.

Based on our current and previous findings, we propose that the mitochondrial ClpP protease is a novel regulator of the in vivo phenotype of VSMCs. Furthermore, we suggest that imipridones, such as TIC10, should be further investigated as potential treatments for aneurysms in humans.

Funding

This work was supported in part by grants from the National Institute on Alcohol Abuse and Alcoholism (F31AA029938 to KMC (ORCID ID:

0000-0002-9461-4032) and AA026086 to SMY (ORCID ID: 0000-0001-9309-0233), National Institute of General Medical Sciences (T32GM008602) to Randy A. Hall, and the National Heart, Lung, and Blood Institute, grants HL144741 and HL165252 to ZL, HL150005 to AR (ORCID ID: 0000-0003-1229-5910) and HL095070 to ASM. The content of this report does not represent the views of the Department of Veterans Affairs or the US Government.

Ethical standards

All animal procedures were approved by the Institutional Animal Care & Use Committee under protocol PROTO201800048. All animal procedures were applied in accordance to the NIH Guide for the Care and Use of Laboratory Animals, and have therefore been performed in accordance with the ethical standards laid down in the 1964 Declaration of Helsinki and its later amendments.

This manuscript does not contain clinical studies or patient data.

CRediT authorship contribution statement

Felipe Paredes: Writing – review & editing, Data curation, Conceptualization. **Holly C. Williams:** Writing – review & editing, Data curation. **Xuesong Liu:** Data curation. **Claire Holden:** Data curation. **Bethany Bogan:** Data curation. **Yu Wang:** Data curation. **Kathryn M. Crotty:** Data curation. **Samantha M. Yeligar:** Resources, Methodology, Funding acquisition, Data curation. **Alvaro A. Elorza:** Data curation. **Zhiyong Lin:** Supervision, Methodology, Funding acquisition. **Amir Rezvan:** Writing – review & editing, Funding acquisition, Data curation, Conceptualization. **Alejandra San Martin:** Writing – review & editing, Writing – original draft, Resources, Project administration, Investigation, Funding acquisition, Data curation, Conceptualization.

Declaration of competing interest

All authors declare that they have no known competing financial interests or personal relationships that could have appeared to influence the work reported in this paper.

The patent “Uses of Hydroimidazopyridopyrimidinone Derivatives for Managing Aneurysms or Other Vascular Conditions or Diseases” is pending to Emory University. This patent submission contains data from the current manuscript. The inventors are Felipe Paredes and Alejandra San Martin.

Data availability

No data was used for the research described in the article.

Appendix A. Supplementary data

Supplementary data to this article can be found online at <https://doi.org/10.1016/j.redox.2024.103203>.

References

- G.K. Owens, M.S. Kumar, B.R. Wamhoff, Molecular regulation of vascular smooth muscle cell differentiation in development and disease, *Physiol. Rev.* 84 (3) (2004) 767–801, <https://doi.org/10.1152/physrev.00041.2003>.
- Y. Liu, S. Sinha, O.G. McDonald, Y. Shang, M.H. Hoofnagle, G.K. Owens, Kruppel-like factor 4 abrogates myocardium-induced activation of smooth muscle gene expression, *J. Biol. Chem.* 280 (10) (2005) 9719–9727, <https://doi.org/10.1074/jbc.M412862200>.
- C.P. Regan, P.J. Adam, C.S. Madsen, G.K. Owens, Molecular mechanisms of decreased smooth muscle differentiation marker expression after vascular injury, *J. Clin. Invest.* 106 (9) (2000) 1139–1147, <https://doi.org/10.1172/JCI10522>.
- M. Salmon, D. Gomez, E. Greene, L. Shankman, G.K. Owens, Cooperative binding of KLF4, pELK-1, and HDAC2 to a G/C repressor element in the SM22alpha promoter mediates transcriptional silencing during SMC phenotypic switching in vivo, *Circ. Res.* 111 (6) (2012) 685–696, <https://doi.org/10.1161/CIRCRESAHA.112.269811>.
- B.R. Wamhoff, M.H. Hoofnagle, A. Burns, S. Sinha, O.G. McDonald, G.K. Owens, A G/C element mediates repression of the SM22alpha promoter within phenotypically modulated smooth muscle cells in experimental atherosclerosis, *Circ. Res.* 95 (10) (2004) 981–988, <https://doi.org/10.1161/01.RES.0000147961.09840.fb>.
- E. Choke, G.W. Cockerill, K. Laing, J. Dawson, W.R. Wilson, I.M. Loftus, M. Thompson, Whole genome-expression profiling reveals a role for immune and inflammatory response in abdominal aortic aneurysm rupture, *Eur. J. Vasc. Endovasc. Surg.* 37 (3) (2009) 305–310, <https://doi.org/10.1016/j.ejvs.2008.11.017>.
- D.C. Guo, H. Pannu, V. Tran-Fadulu, C.L. Papke, R.K. Yu, N. Avidan, S. Bourgeois, A.L. Estrera, H.J. Safi, E. Sparks, D. Amor, L. Ades, V. McConnell, C.E. Wloughby, D. Abuelo, M. Willing, R.A. Lewis, D.H. Kim, S. Scherer, P.P. Tung, C. Ahn, L. M. Buja, C.S. Raman, S.S. Shete, D.M. Milewicz, Mutations in smooth muscle alpha-actin (ACTA2) lead to thoracic aortic aneurysms and dissections, *Nat. Genet.* 39 (12) (2007) 1488–1493, <https://doi.org/10.1038/ng.2007.6>.
- P. Petsohonsakul, M. Furmanik, R. Forsythe, M. Dweck, G.W. Schurink, E. Natour, C. Reutelingsperger, M. Jacobs, B. Mees, L. Schurgers, Role of vascular smooth muscle cell phenotypic switching and calcification in aortic aneurysm formation, *Arterioscler. Thromb. Vasc. Biol.* 39 (7) (2019) 1351–1368, <https://doi.org/10.1161/ATVBAHA.119.312787>.
- K.B. Rombouts, T.A.R. van Merriënboer, J.C.F. Ket, N. Bogunovic, J. van der Velden, K.K. Yeung, The role of vascular smooth muscle cells in the development of aortic aneurysms and dissections, *Eur. J. Clin. Invest.* 52 (4) (2022) e13697, <https://doi.org/10.1111/eci.13697>.
- A. Shalata, M. Mahroom, D.M. Milewicz, G. Limin, F. Kassam, K. Badarna, N. Tarabehi, N. Assy, R. Fell, H. Cohen, M. Nashashibi, A. Livoff, M. Azab, G. Habib, D. Geiger, O. Weissbrod, W. Nseir, Fatal thoracic aortic aneurysm and dissection in a large family with a novel MYLK gene mutation: delineation of the clinical phenotype, *Orphanet J. Rare Dis.* 13 (1) (2018) 41, <https://doi.org/10.1186/s13023-018-0769-7>.
- K.M. van de Luijngaarden, D. Heijtsman, A. Maugeri, M.M. Weiss, H.J. Verhagen, I. J. A, H.T. Bruggenwirth, D. Majoor-Krakauer, First genetic analysis of aneurysm genes in familial and sporadic abdominal aortic aneurysm, *Hum. Genet.* 134 (8) (2015) 881–893, <https://doi.org/10.1007/s00439-015-1567-0>.
- S.E. Wallace, E.S. Regalado, L. Gong, A.L. Janda, D.C. Guo, C.F. Russo, R. J. Kulmacz, N. Hanna, G. Jondeau, C. Boileau, P. Arnaud, K. Lee, S.M. Leal, M. Hannuksela, B. Carlberg, T. Johnston, C. Antolik, E.M. Hostetler, R. Colombo, D. M. Milewicz, MYLK pathogenic variants aortic disease presentation, pregnancy risk, and characterization of pathogenic missense variants, *Genet. Med.* 21 (1) (2019) 144–151, <https://doi.org/10.1038/s41436-018-0038-0>.
- H.G. Zhao, S.J. Fu, M.E. Jiang, [Gene expression difference analysis between abdominal aorta aneurysm and normal abdominal artery], *Zhonghua Wai Ke Za Zhi* 46 (9) (2008) 691–693.
- L. Zhu, R. Vranckx, P. Khau Van Kien, A. Lalande, N. Boisset, F. Mathieu, M. Wegman, L. Glancy, J.M. Gasc, F. Brunotte, P. Bruneval, J.E. Wolf, J.B. Michel, X. Jeunemaitre, Mutations in myosin heavy chain 11 cause a syndrome associating thoracic aortic aneurysm/aortic dissection and patent ductus arteriosus, *Nat. Genet.* 38 (3) (2006) 343–349, <https://doi.org/10.1038/ng1721>.
- H.L. Zu, H.W. Liu, H.Y. Wang, Identification of crucial genes involved in pathogenesis of regional weakening of the aortic wall, *Hereditas* 158 (1) (2021) 35, <https://doi.org/10.1186/s41065-021-00200-1>.
- F. Paredes, H.C. Williams, R.A. Quintana, A. San Martin, Mitochondrial protein Poldip2 (polymerase delta interacting protein 2) controls vascular smooth muscle differentiated phenotype by O-linked GlcNAc (N-acetylglucosamine) transferase-dependent inhibition of a ubiquitin proteasome system, *Circ. Res.* 126 (1) (2020) 41–56, <https://doi.org/10.1161/CIRCRESAHA.119.315932>.
- F. Paredes, K. Sheldon, B. Lassegue, H.C. Williams, E.A. Faidley, G.A. Benavides, G. Torres, F. Sanhueza-Olivares, S.M. Yeligar, K.K. Griendling, V. Darley-Usmar, A. San Martin, Poldip2 is an oxygen-sensitive protein that controls PDH and alphaKGDH lipoylation and activation to support metabolic adaptation in hypoxia and cancer, *Proc. Natl. Acad. Sci. U.S.A.* 115 (8) (2018) 1789–1794, <https://doi.org/10.1073/pnas.1720693115>.
- M.F. Mabanglo, W.A. Houry, Recent structural insights into the mechanism of ClpP protease regulation by AAA+ chaperones and small molecules, *J. Biol. Chem.* 298 (5) (2022) 101781, <https://doi.org/10.1016/j.jbc.2022.101781>.
- P.R. Graves, L.J. Aponte-Collazo, E.M.J. Fennell, A.C. Graves, A.E. Hale, N. Dicheva, L.E. Herring, T.S.K. Gilbert, M.P. East, I.M. McDonald, M.R. Lockett, H. Ashamalla, N.J. Moorman, D.S. Karanewsky, E.J. Iwanowicz, E. Holmuhamedov, L.M. Graves, Mitochondrial protease ClpP is a target for the anticancer compounds ONC201 and related analogues, *ACS Chem. Biol.* 14 (5) (2019) 1020–1029, <https://doi.org/10.1021/acscchembio.9b00222>.
- C.M. Bhamidipati, G.S. Mehta, G. Lu, C.W. Moehle, C. Barbery, P.D. DiMusto, A. Laser, I.L. Kron, G.R. Upchurch Jr., G. Ailawadi, Development of a novel murine model of aortic aneurysms using peri-adventitial elastase, *Surgery* 152 (2) (2012) 238–246, <https://doi.org/10.1016/j.surg.2012.02.010>.
- A. Busch, A. Holm, N. Wagner, S. Ergun, M. Rosenfeld, C. Otto, J. Baur, R. Kellersmann, U. Lorenz, Extra- and intraluminal elastase induce morphologically distinct abdominal aortic aneurysms in mice and thus represent specific subtypes of human disease, *J. Vasc. Res.* 53 (1–2) (2016) 49–57, <https://doi.org/10.1159/000447263>.
- B.P. Dranka, G.A. Benavides, A.R. Diers, S. Giordano, B.R. Zelicson, C. Reily, L. Zou, J.C. Chatham, B.G. Hill, J. Zhang, A. Landar, V.M. Darley-Usmar, Assessing bioenergetic function in response to oxidative stress by metabolic profiling, *Free Radic. Biol. Med.* 51 (9) (2011) 1621–1635, <https://doi.org/10.1016/j.freeradbiomed.2011.08.005>.

- [23] K.S. Seo, J.H. Kim, K.N. Min, J.A. Moon, T.C. Roh, M.J. Lee, K.W. Lee, J.E. Min, Y. M. Lee, KL1333, a novel NAD(+) modulator, improves energy metabolism and mitochondrial dysfunction in MELAS fibroblasts, *Front. Neurol.* 9 (2018) 552, <https://doi.org/10.3389/fneur.2018.00552>.
- [24] X. Kou, H. Ding, L. Li, H. Chao, Caseinolytic protease P (CLPP) activated by ONC201 inhibits proliferation and promotes apoptosis in human epithelial ovarian cancer cells by inducing mitochondrial dysfunction, *Ann. Transl. Med.* 9 (18) (2021) 1463, <https://doi.org/10.21037/atm-21-4321>.
- [25] J. Key, S. Torres-Odio, N.C. Bach, S. Gispert, G. Koepf, M. Reichlmeier, A.P. West, H. Prokisch, P. Freisinger, W.G. Newman, S. Shalev, S.A. Sieber, I. Wittig, G. Auburger, Inactivity of Peptidase ClpP causes primary accumulation of mitochondrial disaggregase ClpX with its interacting nucleoid proteins, and of mtDNA, *Cells* 10 (12) (2021), <https://doi.org/10.3390/cells10123354>.
- [26] G.F. Alencar, K.M. Owsiany, S. Karnewar, K. Sukhvasi, G. Mocchi, A.T. Nguyen, C. M. Williams, S. Shamsuzzaman, M. Mokry, C.A. Henderson, R. Haskins, R.A. Baylis, A.V. Finn, C.A. McNamara, E.R. Zunder, V. Venkata, G. Pasterkamp, J. Bjorkegren, S. Bekiranov, G.K. Owens, Stem cell pluripotency genes Klf4 and Oct4 regulate complex SMC phenotypic changes critical in late-stage atherosclerotic lesion pathogenesis, *Circulation* 142 (21) (2020) 2045–2059, <https://doi.org/10.1161/CIRCULATIONAHA.120.046672>.
- [27] J.M. Miano, E.A. Fisher, M.W. Majesky, Fate and state of vascular smooth muscle cells in atherosclerosis, *Circulation* 143 (21) (2021) 2110–2116, <https://doi.org/10.1161/CIRCULATIONAHA.120.049922>.
- [28] H. Pan, C. Xue, B.J. Auerbach, J. Fan, A.C. Bashore, J. Cui, D.Y. Yang, S. B. Trignano, W. Liu, J. Shi, C.O. Ihuegbu, E.C. Bush, J. Worley, L. Vlahos, P. Laise, R.A. Solomon, E.S. Connolly, A. Califano, P.A. Sims, H. Zhang, M. Li, M.P. Reilly, Single-cell genomics reveals a novel cell state during smooth muscle cell phenotypic switching and potential therapeutic targets for atherosclerosis in mouse and human, *Circulation* 142 (21) (2020) 2060–2075, <https://doi.org/10.1161/CIRCULATIONAHA.120.048378>.
- [29] S.G. Kang, M.N. Dimitrova, J. Ortega, A. Ginsburg, M.R. Maurizi, Human mitochondrial ClpP is a stable heptamer that assembles into a tetradecamer in the presence of ClpX, *J. Biol. Chem.* 280 (42) (2005) 35424–35432, <https://doi.org/10.1074/jbc.M507240200>.
- [30] N. Al-Furokhan, A. Ianni, H. Nolte, S. Holper, M. Kruger, S. Wanrooij, T. Braun, ClpX stimulates the mitochondrial unfolded protein response (UPR^{mt}) in mammalian cells, *Biochim. Biophys. Acta* 1853 (10 Pt A) (2015) 2580–2591, <https://doi.org/10.1016/j.bbamcr.2015.06.016>.
- [31] J.G. Ryall, S. Dell'Orso, A. Derfoul, A. Juan, H. Zare, X. Feng, D. Clermont, M. Koulis, G. Gutierrez-Cruz, M. Fulco, V. Sartorelli, The NAD(+) dependent SIRT1 deacetylase translates a metabolic switch into regulatory epigenetics in skeletal muscle stem cells, *Cell Stem Cell* 16 (2) (2015) 171–183, <https://doi.org/10.1016/j.stem.2014.12.004>.
- [32] K. Huang, Z.Q. Yan, D. Zhao, S.G. Chen, L.Z. Gao, P. Zhang, B.R. Shen, H.C. Han, Y. X. Qi, Z.L. Jiang, SIRT1 and FOXO mediate contractile differentiation of vascular smooth muscle cells under cyclic stretch, *Cell. Physiol. Biochem.* 37 (5) (2015) 1817–1829, <https://doi.org/10.1159/000438544>.
- [33] U. Kilic, O. Gok, A. Bacaksiz, M. Izmirlil, B. Elibol-Can, O. Uysal, SIRT1 gene polymorphisms affect the protein expression in cardiovascular diseases, *PLoS One* 9 (2) (2014) e90428, <https://doi.org/10.1371/journal.pone.0090428>.
- [34] M. Izmirlil, O. Goktekin, A. Bacaksiz, O. Uysal, U. Kilic, The effect of the SIRT1 2827 A>G polymorphism, resveratrol, exercise, age and occupation in Turkish population with cardiovascular disease, *Anatol. J. Cardiol.* 15 (2) (2015) 103–106, <https://doi.org/10.5152/akd.2014.5214>.
- [35] H. Brotz-Oesterhelt, D. Beyer, H.P. Kroll, R. Endermann, C. Ladel, W. Schroeder, B. Hinzen, S. Raddatz, H. Paulsen, K. Henninger, J.E. Bandow, H.G. Sahl, H. Labischinski, Dysregulation of bacterial proteolytic machinery by a new class of antibiotics, *Nat. Med.* 11 (10) (2005) 1082–1087, <https://doi.org/10.1038/nm1306>.
- [36] J. Ishizawa, S.F. Zarabi, R.E. Davis, O. Halgas, T. Nii, Y. Jitkova, R. Zhao, J. St-Germain, L.E. Heese, G. Egan, V.R. Ruvolo, S.H. Barghout, Y. Nishida, R. Hurren, W. Ma, M. Gronda, T. Link, K. Wong, M. Mabanglo, K. Kojima, G. Borthakur, N. MacLean, M.C.J. Ma, A.B. Leber, M.D. Minden, W. Houry, H. Kantarjian, M. Stogniew, B. Raught, E.F. Pai, A.D. Schimmer, M. Andreeff, Mitochondrial ClpP-mediated proteolysis induces selective cancer cell lethality, *Cancer Cell* 35 (5) (2019) 721–737 e9, <https://doi.org/10.1016/j.ccell.2019.03.014>.
- [37] W.E. Balch, R.I. Morimoto, A. Dillin, J.W. Kelly, Adapting proteostasis for disease intervention, *Science* 319 (5865) (2008) 916–919, <https://doi.org/10.1126/science.1141448>.
- [38] N. Sabath, F. Levy-Adam, A. Younis, K. Rozales, A. Meller, S. Hadar, S. Soueid-Baumgarten, R. Shalgi, Cellular proteostasis decline in human senescence, *Proc. Natl. Acad. Sci. U.S.A.* 117 (50) (2020) 31902–31913, <https://doi.org/10.1073/pnas.2018138117>.
- [39] J. Campisi, P. Kapahi, G.J. Lithgow, S. Melov, J.C. Newman, E. Verdin, From discoveries in ageing research to therapeutics for healthy ageing, *Nature* 571 (7764) (2019) 183–192, <https://doi.org/10.1038/s41586-019-1365-2>.
- [40] C.L. Klaiaps, G.G. Jayaraj, F.U. Hartl, Pathways of cellular proteostasis in aging and disease, *J. Cell Biol.* 217 (1) (2018) 51–63, <https://doi.org/10.1083/jcb.201709072>.
- [41] C.A. Goard, A.D. Schimmer, Mitochondrial matrix proteases as novel therapeutic targets in malignancy, *Oncogene* 33 (21) (2014) 2690–2699, <https://doi.org/10.1038/onc.2013.228>.
- [42] E. Hofsetz, F. Demir, K. Szczepanowska, A. Kukat, J.N. Kizhakkedathu, A. Trifunovic, P.F. Huesgen, The mouse Heart mitochondria N terminome provides insights into ClpXP-mediated proteolysis, *Mol. Cell. Proteomics* 19 (8) (2020) 1330–1345, <https://doi.org/10.1074/mcp.RA120.002082>.
- [43] P.R. Strack, E.J. Brodie, H. Zhan, V.J. Schuenemann, L.J. Valente, T. Saiyed, B. R. Lowth, L.M. Anglely, M.A. Perugini, K. Zeth, K.N. Truscott, D.A. Dougan, Polymerase delta-interacting protein 38 (PDIP38) modulates the stability and activity of the mitochondrial AAA+ protease CLPXP, *Commun. Biol.* 3 (1) (2020) 646, <https://doi.org/10.1038/s42003-020-01358-6>.
- [44] E. Hofsetz, The Role of SDHA in the Tissue-specific Regulation of Metabolism and Proteomic Approaches to Identify Novel ClpXP Substrates, 2020. Dissertation, <https://kups.uni-koeln.de/10493/>.
- [45] S. Kitazawa, S. Ebara, A. Ando, Y. Baba, Y. Satomi, T. Soga, T. Hara, Succinate dehydrogenase B-deficient cancer cells are highly sensitive to bromodomain and extra-terminal inhibitors, *Oncotarget* 8 (17) (2017) 28922–28938, <https://doi.org/10.18632/oncotarget.15959>.
- [46] J. Hirst, Mitochondrial complex I, *Annu. Rev. Biochem.* 82 (2013) 551–575, <https://doi.org/10.1146/annurev-biochem-070511-103700>.
- [47] K. Szczepanowska, K. Senft, J. Heidler, M. Herholz, A. Kukat, M.N. Hohne, E. Hofsetz, C. Becker, S. Kaspar, H. Giese, K. Zwicker, S. Guerrero-Castillo, L. Baumann, J. Kauppila, A. Rummyantseva, S. Muller, C.K. Frese, U. Brandt, J. Riemer, I. Wittig, A. Trifunovic, A salvage pathway maintains highly functional respiratory complex I, *Nat. Commun.* 11 (1) (2020) 1643, <https://doi.org/10.1038/s41467-020-15467-7>.
- [48] S.L. Olson, A.M. Panthofer, W. Blackwelder, M.L. Terrin, J.A. Curci, B.T. Baxter, F. A. Weaver, D.J.A. Scott, K.E. Porter, Progressive development of aberrant aortic aneurysm clinical trial, role of volume in small abdominal aortic aneurysm surveillance, *J. Vasc. Surg.* 75 (4) (2022) 1260–1267 e3, <https://doi.org/10.1016/j.jvs.2021.09.046>.
- [49] T. Shirasu, H. Takagi, J. Yasuhara, T. Kuno, K.C. Kent, W.D. Clouse, Smaller size is more suitable for pharmacotherapy among undersized abdominal aortic aneurysm: a systematic review and meta-analysis, *Vasc. Med.* (2021) 1358863X211061603, <https://doi.org/10.1177/1358863X211061603>.
- [50] K. Riches, E. Clark, R.J. Helliwell, T.G. Angelini, K.E. Hemmings, M.A. Bailey, K. I. Bridge, D.J.A. Scott, K.E. Porter, Progressive development of aberrant smooth muscle cell phenotype in abdominal aortic aneurysm disease, *J. Vasc. Res.* 55 (1) (2018) 35–46, <https://doi.org/10.1159/000484088>.
- [51] A. Busch, H. Hartmann, C. Grimm, S. Ergun, R. Kickuth, C. Otto, R. Kellersmann, U. Lorenz, Heterogeneous histomorphology, yet homogeneous vascular smooth muscle cell dedifferentiation, characterize human aneurysm disease, *J. Vasc. Surg.* 66 (5) (2017) 1553–1564 e6, <https://doi.org/10.1016/j.jvs.2016.07.129>.
- [52] C.H. Lai, C.W. Chang, F.T. Lee, C.H. Kuo, J.H. Hsu, C.P. Liu, H.L. Wu, J.L. Yeh, Targeting vascular smooth muscle cell dysfunction with xanthine derivative KMUP-3 inhibits abdominal aortic aneurysm in mice, *Atherosclerosis* 297 (2020) 16–24, <https://doi.org/10.1016/j.atherosclerosis.2020.01.029>.
- [53] E.S. Liang, W. Cheng, R.X. Yang, W.W. Bai, X. Liu, Y.X. Zhao, Peptidyl-prolyl isomerase Pin1 deficiency attenuates angiotensin II-induced abdominal aortic aneurysm formation in ApoE(-/-) mice, *J. Mol. Cell. Cardiol.* 114 (2018) 334–344, <https://doi.org/10.1016/j.yjmcc.2017.12.006>.
- [54] L. Zhong, X. He, X. Si, H. Wang, B. Li, Y. Hu, M. Li, X. Chen, W. Liao, Y. Liao, J. Bin, SM22alpha (smooth muscle 22 alpha) prevents aortic aneurysm formation by inhibiting smooth muscle cell phenotypic switching through suppressing reactive oxygen species/NF-kappaB (nuclear factor-kappaB), *Arterioscler. Thromb. Vasc. Biol.* 39 (1) (2019) e10–e25, <https://doi.org/10.1161/ATVBAHA.118.311917>.
- [55] H. Peng, K. Zhang, Z. Liu, Q. Xu, B. You, C. Li, J. Cao, H. Zhou, X. Li, J. Chen, G. Cheng, R. Shi, G. Zhang, VPO1 modulates vascular smooth muscle cell phenotypic switch by activating extracellular signal-regulated kinase 1/2 (ERK 1/2) in abdominal aortic aneurysms, *J. Am. Heart Assoc.* 7 (17) (2018) e010069, <https://doi.org/10.1161/JAHA.118.010069>.
- [56] X. Qin, L. He, M. Tian, P. Hu, J. Yang, H. Lu, W. Chen, X. Jiang, C. Zhang, J. Gao, M. Chen, L.S. Weinstein, Y. Zhang, W. Zhang, Smooth muscle-specific Galpha deletion exaggerates angiotensin II-induced abdominal aortic aneurysm formation in mice in vivo, *J. Mol. Cell. Cardiol.* 132 (2019) 49–59, <https://doi.org/10.1016/j.yjmcc.2019.05.002>.
- [57] S. Wang, C. Jia, TRPV1 inhibits smooth muscle cell phenotype switching in a mouse model of abdominal aortic aneurysm, *Channels* 14 (1) (2020) 59–68, <https://doi.org/10.1080/19336950.2020.1730020>.
- [58] K. Mukherjee, J.M. Gitlin, C.D. Loftin, Effectiveness of cyclooxygenase-2 inhibition in limiting abdominal aortic aneurysm progression in mice correlates with a differentiated smooth muscle cell phenotype, *J. Cardiovasc. Pharmacol.* 60 (6) (2012) 520–529, <https://doi.org/10.1097/FJC.0b013e318270b968>.
- [59] C.W. Moehle, C.M. Bhamidipati, M.R. Alexander, G.S. Mehta, J.N. Irvine, M. Salmon, G.R. Upchurch Jr., I.L. Kron, G.K. Owens, G. Ailawadi, Bone marrow-derived MCP1 required for experimental aortic aneurysm formation and smooth muscle phenotypic modulation, *J. Thorac. Cardiovasc. Surg.* 142 (6) (2011) 1567–1574, <https://doi.org/10.1016/j.jtcvs.2011.07.053>.
- [60] M. Salmon, W.F. Johnston, A. Woo, N.H. Pope, G. Su, G.R. Upchurch Jr., G. K. Owens, G. Ailawadi, KLF4 regulates abdominal aortic aneurysm morphology and deletion attenuates aneurysm formation, *Circulation* 128 (11 Suppl 1) (2013) S163–S174, <https://doi.org/10.1161/CIRCULATIONAHA.112.000238>.
- [61] A. Malashicheva, D. Kostina, A. Kostina, O. Irtuga, I. Voronkina, L. Smagina, E. Ignatieva, N. Gavriluk, V. Uspensky, O. Moiseeva, J. Vaage, A. Kostareva, Phenotypic and functional changes of endothelial and smooth muscle cells in thoracic aortic aneurysms, *Int. J. Vasc. Med.* 2016 (2016) 3107879, <https://doi.org/10.1155/2016/3107879>.
- [62] N. Mao, T. Gu, E. Shi, G. Zhang, L. Yu, C. Wang, Phenotypic switching of vascular smooth muscle cells in animal model of rat thoracic aortic aneurysm, *Interact. Cardiovasc. Thorac. Surg.* 21 (1) (2015) 62–70, <https://doi.org/10.1093/icvts/ivv074>.

- [63] A. Forte, A. Della Corte, M. Grossi, C. Bancone, C. Maiello, U. Galderisi, M. Cipollaro, Differential expression of proteins related to smooth muscle cells and myofibroblasts in human thoracic aortic aneurysm, *Histol. Histopathol.* 28 (6) (2013) 795–803, <https://doi.org/10.14670/HH-28.795>.
- [64] E. Branchetti, P. Poggio, R. Sainger, E. Shang, J.B. Grau, B.M. Jackson, E.K. Lai, M. S. Parmacek, R.C. Gorman, J.H. Gorman, J.E. Bavaria, G. Ferrari, Oxidative stress modulates vascular smooth muscle cell phenotype via CTGF in thoracic aortic aneurysm, *Cardiovasc. Res.* 100 (2) (2013) 316–324, <https://doi.org/10.1093/cvr/cvt205>.
- [65] R. Liu, L. Lo, A.J. Lay, Y. Zhao, K.K. Ting, E.N. Robertson, A.G. Sherrah, S. Jarrah, H. Li, Z. Zhou, B.D. Hambly, D.R. Richmond, R.W. Jeremy, P.G. Bannon, M. A. Vadas, J.R. Gamble, ARHGAP18 protects against thoracic aortic aneurysm formation by mitigating the synthetic and proinflammatory smooth muscle cell phenotype, *Circ. Res.* 121 (5) (2017) 512–524, <https://doi.org/10.1161/CIRCRESAHA.117.310692>.
- [66] A. Chiarini, F. Onorati, M. Marconi, A. Pasquali, C. Patuzzo, A. Malashicheva, O. Irtyega, G. Faggian, P.F. Pignatti, E. Trabetti, U. Armato, I. Dal Pra, Studies on sporadic non-syndromic thoracic aortic aneurysms: 1. Deregulation of Jagged/Notch 1 homeostasis and selection of synthetic/secretor phenotype smooth muscle cells, *Eur. J. Prev. Cardiol.* 25 (1 suppl) (2018) 42–50, <https://doi.org/10.1177/2047487318759119>.
- [67] J. Huang, E.C. Davis, S.L. Chapman, M. Budatha, L.Y. Marmorstein, R.A. Word, H. Yanagisawa, Fibulin-4 deficiency results in ascending aortic aneurysms: a potential link between abnormal smooth muscle cell phenotype and aneurysm progression, *Circ. Res.* 106 (3) (2010) 583–592, <https://doi.org/10.1161/CIRCRESAHA.109.207852>.
- [68] M. Nogi, K. Satoh, S. Sunamura, N. Kikuchi, T. Satoh, R. Kurosawa, J. Omura, M. Elias-Al-Mamun, M. Abdul Hai Siddique, K. Numano, S. Kudo, S. Miyata, M. Akiyama, K. Kumagai, S. Kawamoto, Y. Saiki, H. Shimokawa, Small GTP-binding protein GDP dissociation stimulator prevents thoracic aortic aneurysm formation and rupture by phenotypic preservation of aortic smooth muscle cells, *Circulation* 138 (21) (2018) 2413–2433, <https://doi.org/10.1161/CIRCULATIONAHA.118.035648>.
- [69] G. Ailawadi, C.W. Moehle, H. Pei, S.P. Walton, Z. Yang, I.L. Kron, C.L. Lau, G. K. Owens, Smooth muscle phenotypic modulation is an early event in aortic aneurysms, *J. Thorac. Cardiovasc. Surg.* 138 (6) (2009) 1392–1399, <https://doi.org/10.1016/j.jtcvs.2009.07.075>.
- [70] J.E. Allen, R.N. Crowder, W.S. El-Deiry, First-in-Class small molecule ONC201 induces DR5 and cell death in tumor but not normal cells to provide a wide therapeutic index as an anti-cancer agent, *PLoS One* 10 (11) (2015) e0143082, <https://doi.org/10.1371/journal.pone.0143082>.
- [71] J.E. Allen, G. Kringsfeld, P.A. Mayes, L. Patel, D.T. Dicker, A.S. Patel, N.G. Dolloff, E. Messaris, K.A. Scata, W. Wang, J.Y. Zhou, G.S. Wu, W.S. El-Deiry, Dual inactivation of Akt and ERK by TIC10 signals Foxo3a nuclear translocation, TRAIL gene induction, and potent antitumor effects, *Sci. Transl. Med.* 5 (171) (2013) 171ra17, <https://doi.org/10.1126/scitranslmed.3004828>.
- [72] J.E. Allen, V.V. Prabhu, M. Talekar, A.P. van den Heuvel, B. Lim, D.T. Dicker, J. L. Fritz, A. Beck, W.S. El-Deiry, Genetic and pharmacological screens converge in identifying FLIP, BCL2, and IAP proteins as key regulators of sensitivity to the TRAIL-inducing anticancer agent ONC201/TIC10, *Cancer Res.* 75 (8) (2015) 1668–1674, <https://doi.org/10.1158/0008-5472.CAN-14-2356>.
- [73] L. Cheng, Y.Y. Liu, P.H. Lu, Y. Peng, Q. Yuan, X.S. Gu, Y. Jin, M.B. Chen, X.M. Bai, Identification of DNA-PKcs as a primary resistance factor of TIC10 in hepatocellular carcinoma cells, *Oncotarget* 8 (17) (2017) 28385–28394, <https://doi.org/10.18632/oncotarget.16073>.
- [74] Y. Feng, J. Zhou, Z. Li, Y. Jiang, Y. Zhou, Small molecular trail inducer ONC201 induces death in Lung cancer cells: a preclinical study, *PLoS One* 11 (9) (2016) e0162133, <https://doi.org/10.1371/journal.pone.0162133>.
- [75] A.A. Hayes-Jordan, X. Ma, B.A. Menegaz, S.E. Lamhamedi-Cherradi, C.V. Kingsley, J.A. Benson, P.E. Camacho, J.A. Ludwig, C.R. Lockworth, G.E. Garcia, S.L. Craig, Efficacy of ONC201 in desmoplastic small round cell tumor, *Neoplasia* 20 (5) (2018) 524–532, <https://doi.org/10.1016/j.neo.2018.02.006>.
- [76] J. Ishizawa, K. Kojima, D. Chachad, P. Ruvolo, V. Ruvolo, R.O. Jacamo, G. Borthakur, H. Mu, Z. Zeng, Y. Tabe, J.E. Allen, Z. Wang, W. Ma, H.C. Lee, R. Orlovski, D. Sarbassov dos, P.L. Lorenzi, X. Huang, S.S. Neelapu, T. McDonnell, R.N. Miranda, M. Wang, H. Kantarjian, M. Konopleva, R.E. Davis, M. Andreeff, ATF4 induction through an atypical integrated stress response to ONC201 triggers p53-independent apoptosis in hematological malignancies, *Sci. Signal.* 9 (415) (2016) ra17, <https://doi.org/10.1126/scisignal.aac4380>.
- [77] C.L. Kline, A.P. Van den Heuvel, J.E. Allen, V.V. Prabhu, D.T. Dicker, W.S. El-Deiry, ONC201 kills solid tumor cells by triggering an integrated stress response dependent on ATF4 activation by specific eIF2alpha kinases, *Sci. Signal.* 9 (415) (2016) ra18, <https://doi.org/10.1126/scisignal.aac4374>.
- [78] T. Nii, V.V. Prabhu, V. Ruvolo, N. Madhukar, R. Zhao, H. Mu, L. Heese, Y. Nishida, K. Kojima, M.J. Garnett, U. McDermott, C.H. Benes, N. Charter, S. Deacon, O. Elemento, J.E. Allen, W. Oster, M. Stogniew, J. Ishizawa, M. Andreeff, Imipridone ONC212 activates orphan G protein-coupled receptor GPR132 and integrated stress response in acute myeloid leukemia, *Leukemia* 33 (12) (2019) 2805–2816, <https://doi.org/10.1038/s41375-019-0491-z>.
- [79] V.V. Prabhu, J.E. Allen, D.T. Dicker, W.S. El-Deiry, Small-molecule ONC201/TIC10 targets chemotherapy-resistant colorectal cancer stem-like cells in an akt/foxo3a/TRAIL-dependent manner, *Cancer Res.* 75 (7) (2015) 1423–1432, <https://doi.org/10.1158/0008-5472.CAN-13-3451>.
- [80] V.V. Prabhu, M.K. Talekar, A.R. Lulla, C.L.B. Kline, L. Zhou, J. Hall, A.P.J. Van den Heuvel, D.T. Dicker, J. Babar, S.A. Grupp, M.J. Garnett, U. McDermott, C.H. Benes, J.J. Pu, D.F. Claxton, N. Khan, W. Oster, J.E. Allen, W.S. El-Deiry, Single agent and synergistic combinatorial efficacy of first-in-class small molecule imipridone ONC201 in hematological malignancies, *Cell Cycle* 17 (4) (2018) 468–478, <https://doi.org/10.1080/15384101.2017.1403689>.
- [81] M.D. Ralff, C.L.B. Kline, O.C. Kucukkase, J. Wagner, B. Lim, D.T. Dicker, V. V. Prabhu, W. Oster, W.S. El-Deiry, ONC201 demonstrates antitumor effects in both triple-negative and non-triple-negative breast cancers through TRAIL-dependent and TRAIL-independent mechanisms, *Mol. Cancer Therapeut.* 16 (7) (2017) 1290–1298, <https://doi.org/10.1158/1535-7163.MCT-17-0121>.
- [82] J. Wagner, C.L. Kline, L. Zhou, K.S. Campbell, A.W. MacFarlane, A.J. Olszanski, K. Q. Cai, H.H. Hensley, E.A. Ross, M.D. Ralff, A. Zloza, C.B. Chesson, J.H. Newman, H. Kaufman, J. Bertino, M. Stein, W.S. El-Deiry, Dose intensification of TRAIL-inducing ONC201 inhibits metastasis and promotes intratumoral NK cell recruitment, *J. Clin. Invest.* 128 (6) (2018) 2325–2338, <https://doi.org/10.1172/JCI96711>.
- [83] J. Wagner, C.L. Kline, L. Zhou, V. Khazak, W.S. El-Deiry, Anti-tumor effects of ONC201 in combination with VEGF-inhibitors significantly impacts colorectal cancer growth and survival in vivo through complementary non-overlapping mechanisms, *J. Exp. Clin. Cancer Res.* 37 (1) (2018) 11, <https://doi.org/10.1186/s13046-018-0671-0>.
- [84] J. Wang, H. Wang, L.Y. Wang, D. Cai, Z. Duan, Y. Zhang, P. Chen, J.X. Zou, J. Xu, X. Chen, H.J. Kung, H.W. Chen, Silencing the epigenetic silencer KDM4A for TRAIL and DR5 simultaneous induction and antitumor therapy, *Cell Death Differ.* 23 (11) (2016) 1886–1896, <https://doi.org/10.1038/cdd.2016.92>.
- [85] Q. Zhang, H. Wang, L. Ran, Z. Zhang, R. Jiang, The preclinical evaluation of TIC10/ONC201 as an anti-pancreatic cancer agent, *Biochem. Biophys. Res. Commun.* 476 (4) (2016) 260–266, <https://doi.org/10.1016/j.bbrc.2016.05.106>.
- [86] R. Zhao, Y. Li, S. Gorantla, L.Y. Poluektova, H. Lin, F. Gao, H. Wang, J. Zhao, J. C. Zheng, Y. Huang, Small molecule ONC201 inhibits HIV-1 replication in macrophages via FOXO3a and TRAIL, *Antivir. Res.* 168 (2019) 134–145, <https://doi.org/10.1016/j.antiviral.2019.05.015>.